MINERALOGICAL MAGAZINE, JUNE 1983, VOL. 47, PP. 201-208

The dependence of alumina and silica contents on the extent of alteration of weathered ilmenites from Western Australia

M. T. FROST, I. E. GREY,* I. R. HARROWFIELD, AND K. MASON

CSIRO Division of Mineral Chemistry, P.O. Box 124, Port Melbourne, Victoria 3207, Australia

ABSTRACT. The distribution of the minor impurities, aluminium and silicon, between co-existing phases in altered ilmenite grains from three Western Australian localities has been investigated using SEM and electron-microprobe analyses. A striking dependence of the impurity levels on the Ti/(Ti+Fe) fraction is observed. For compositions with Ti/(Ti+Fe) between 0.45 and 0.60, i.e. between ferrian-ilmenite and pseudorutile, the impurity content is virtually independent of Ti/(Ti+Fe), and is very low (0.2 wt. % Al_2O_3. 0.05 wt. % SiO_2). For compositions between those of rutile and pseudorutile, there is a direct correlation between the impurity contents and the Ti content of the alteration phase. The impurity levels increase with increasing Ti/(Ti+Fe) to about 3 wt. % Al_2O_3 and 1 wt. % SiO_2 for compositions close to TiO_2. Thus during the latter stages of ilmenite alteration, alumina and silica are extracted from the ambient environment and are coprecipitated with, or adsorbed on to, the alteration products. The observed dependence of the alumina and silica contents on extent of alteration is consistent with a two-stage alteration mechanism earlier proposed (Grey and Reid, 1975).

THE production of pigment-grade titanium dioxide by the chloride route has traditionally required rutile as a feedstock because of its relatively high purity, $>95\%$ TiO_2. However, as reserves of the natural mineral decline, producers have turned to synthetic equivalents derived from the abundant mineral ilmenite. Commercial ilmenite-upgrading processes that are currently in production include a direct-reduction and leach process operated by Associated Minerals Consolidated at Capel, Western Australia, and the Benilite hydrochloric acid leach process operated by Kerr-McGee in the USA and Taiwan. A problem common to most beneficiation routes is their inability to reduce significantly the levels of alumina and silica impurities in ilmenite (0.5 to 1% Al_2O_3 and SiO_2). Selective leaching processes only partially remove alumina and have negligible attack on the silica. These impurities arise both from separate aluminosilicate minerals such as staurolite, tourmaline, and kyanite, and from alteration phases within the ilmenite grains. Improved wet- and dry-separation techniques for heavy-mineral concentrates have practically eliminated the former impurity source, but very little is known of the latter type of impurity. As part of a study on the nature of the intra-grain alumina and silica impurities, we have carried out a scanning electron microscopy (SEM) and electron microprobe analytical study on three different ilmenite samples from Western Australian localities, the results of which are reported here.

* Author to whom correspondence is to be addressed.

Experimental

The samples studied were commercial ilmenite concentrates derived from heavy mineral beach sand deposits on the south-west coast of Western Australia. Samples of sulphate-grade ilmenite derived from the 90-foot (YE-90) and 150-foot (YE-150) strand lines of the Yoganup Extended mine at Capel, 150 km south of Perth, were supplied by Westralian Sands Ltd. (WSL), and a sample of altered ilmenite from Eneabba, 200 km north of Perth, was supplied by Associated Minerals Consolidated (AMC). Chemical analyses for the three samples are given in Table I.

Phases were identified by grinding samples to $-45\ \mu m$, and obtaining X-ray diffraction patterns using Cu-$K\alpha$ radiation, scanning at $1°\ min^{-1}$ on a Philips diffractometer fitted with a graphite monochromator. Where accurate lattice parameters were required, silicon was added as an internal standard and a scan rate of $0.25°\ min^{-1}$ was used.

Samples for SEM and electron microprobe analyses were mounted in epoxy resin doped with graphite and polished at a final cutting-paste size of $1\ \mu m$. They were first examined in a JEOL JSM-U3 SEM fitted with a Robinson-type large-area, scintillation back-scattered electron (BSE) detector (Robinson, 1975), and energy-dispersive X-ray analysis system (EDS), and then analysed for Fe, Ti, Al, and Si in a JEOL JXA-50A electron microprobe using rutile, spinel ($MgAl_2O_4$), hematite, and wollastonite as standards. Generally, composite grains showing at least two different alteration phases were

selected for analysis to obtain a quantitative measure of the change in the minor element distributions associated with the change in the Ti/(Ti + Fe) atomic fraction in the co-existing phases. Point analyses were obtained for at least two separate regions of each phase type.

To obtain statistically significant information on the relationship between alumina, silica impurity levels, and inter- and intra-grain Fe and Ti contents (reflecting the extent of the weathering), an automated modal analysis procedure was developed for the JXA-50A microprobe. In this procedure the grain mounts were scanned automatically along a series of parallel lines, 4200 μm long and separated by 200 μm to ensure that an independent set of grains was encountered along each line. Wavelength dispersive analyses were carried out with two crystal spectrometers; one for Al and Si and the other for Fe and Ti. For each line scan, a 1/32 s count for titanium was made at 3 μm intervals, to distinguish Ti-rich phases from the plastic matrix. An index number, preset at one, was increased by unit steps each time an intervening region of plastic was encountered. As the grains were mostly separated by distances greater than 3 μm, this index served to group together the analyses belonging to individual grains. By this method, both inter-grain and intra-grain compositional variations were characterized. At every tenth 3 μm step, the scan was arrested and analyses for Ti, Fe, Al, and Si were made, using 4-s counting times. On average, about ninety full analyses, involving about thirty grains, were obtained from each line scan. The output information included the grain index number, the weight percents of each element (as oxides), and the Ti/(Ti + Fe) atomic fraction. The number of points analysed was 935 from 213 grains of Eneabba ilmenite, 880 from 363 grains of YE-90, and 460 from 203 grains of YE-150 ilmenite.

Previous studies in this laboratory have shown that when such large numbers of point analyses of ilmenite alteration phases are made, then the frequency of occurrence of a particular analysis (or range of analyses) is a close approximation to the volume fraction of the phase with the specified analysis, or to its weight fraction where all phases present have similar densities. This is because the majority of altered ilmenite grains have essentially random distributions of alteration phases. Thus the information obtained from the automated scans also provided the basis for determining approximate weight fractions of the various alteration phases.

A number of grains of the Eneabba sample, which were confirmed to be homogeneous in the SEM (BSE image) were subjected to microprobe analyses to determine the Ti/(Ti + Fe) fraction and then excavated from the grain mount and examined by single-crystal XRD (precession and Weissenberg) techniques to determine the phases present. In this way a picture was built up of the phase changes occurring in individual grains at the different stages of alteration.

This approach is subject to the limitation that the SEM examination is confined to the cross-section exposed in the grain mount whereas the XRD pattern corresponds to the whole grain. Thus ambiguities in interpretation may arise when two or more phases are identified by XRD, i.e. the phases may be intergrown on such a fine scale that they cannot be resolved in the SEM and they appear as a homogeneous single phase with Ti/(Ti + Fe) corresponding to the average composition of the mixture, or, alternatively, coarse mixtures (as in fig. 1) of the phases are distributed throughout the grain but the exposed cross-section cuts through only one of the phases and the measured Ti/(Ti + Fe) corresponds to this phase only. There is a low statistical probability of the latter situation, particularly if the grains are sectioned close to their centres, and if enough grains are examined a consistent picture of the alteration process should emerge.

Results and discussion

General characterization. From the chemical analyses for the three ilmenite samples, Table I, it is seen that the Eneabba sample is considerably more altered than those from the Capel area, as reflected in the higher TiO_2 and very low FeO figures. The material from the 150-foot strand is less altered than that from the 90-foot strand, having a higher atomic ratio of ferrous to ferric iron, 0.69, than that for the latter, 0.49. The levels of Al_2O_3 and SiO_2 impurities in YE-150 are somewhat higher than those for YE-90.

TABLE I. *Chemical analyses* of ilmenite samples (wt. %)*

	Eneabba	YE-90	YE-150
TiO_2	59.2	56.4	56.5
Fe_2O_3	29.9	27.0	23.9
FeO	4.6	12.0	14.8
Al_2O_3	0.57	0.49	1.1
SiO_2	1.1	0.70	0.97
MnO	1.2	1.4	1.4
MgO	0.21	n.a.	n.a.
ZrO_2	1.0	0.17	0.13
V_2O_5	0.16	n.a.	n.a.
Cr_2O_3	0.15	0.03	0.04
P_2O_5	0.02	0.05	0.04
LOI (1000 °C)	1.4	1.6	1.2

* Analysed by AMC and WSL.

A powder XRD pattern for the Eneabba sample showed pseudorutile as the dominant phase, together with minor amounts of ilmenite and rutile and trace amounts of anatase, hematite, and quartz. The two Capel samples differ markedly in their phase assemblages. YE-90 is a typical altered ilmenite, with a pseudorutile–ilmenite–rutile assemblage, whereas YE-150 comprises the unusual assemblage (ferrian-ilmenite)–(H-239)–rutile together with small amounts of geothite, pseudorutile, hematite, and anatase. H-239 is a metastable phase with composition close to $Fe_2Ti_3O_9$, prepared by heating ilmenite or pseudorutile in air at tempera-

tures below 800 °C (Grey and Reid, 1972; Grey *et al.*, 1973). The ferrian-ilmenite was concentrated magnetically, using a Cook isodynamic separator. For YE-150, 23 wt. % of strongly magnetic material separated in the 0.05 amp. fraction compared with only 2 wt. % for YE-90. A refinement of lattice parameters for the ferrian-ilmenite in the magnetic fraction gave $a = 5.079(1)$, $c = 13.937(9)$ Å. This phase has been independently confirmed in Capel altered ilmenite samples by Wort and Jones (1981) from XRD studies on magnetically orientated grains. Further studies on the occurrence of H-239 and ferrian-ilmenite in YE-150 will be subsequently reported.

The single-grain XRD studies on the Eneabba sample showed that essentially single-phase pseudorutile occurred over a range of Ti/(Ti+Fe) values, from 0.6 to 0.7 (i.e. ~60–70 wt. % TiO_2).* This is in accord with the studies of Dyadchenko and Khatuntseva (1960) who found that pseudorutile (called arizonite by these authors) had a range of composition given by $Fe_2O_3 \cdot nTiO_2 \cdot mH_2O$, $n = 3$–5, $m = 1$–2. Our single-grain XRD studies showed that a small amount of hematite, in topotactic relation to pseudorutile, always occurred in grains with $0.6 < Ti/(Ti+Fe) < 0.7$.

Grains with Ti/(Ti+Fe) ratios in the range 0.5 to 0.6 were consistently found to comprise two-phase mixtures of pseudorutile plus ilmenite whereas the XRD patterns of grains with Ti/(Ti+Fe) > 0.7 showed two-phase mixtures of pseudorutile plus rutile. Occasionally a small amount of H-239, in topotactic relation to ilmenite, was detected in precession photographs of grains with $0.5 < Ti/(Ti+Fe) < 0.6$.

The single-grain XRD studies thus confirm that alteration of Eneabba ilmenite proceeds through the formation of a single intermediate phase with an extended range of composition and that the intervening, predominantly two-phase, regions comprise intergrowths on a fine scale, that appear homogeneous in a SEM. The observed two-phase regions correspond compositionally to the ilmenite alteration stages called hydrated ilmenite and leucoxene by Dyadchenko and Khatuntseva (1960), and in this paper we retain the terminology used by the Russian workers.

* The molecular weights of TiO_2 (79.9) and $FeO_{1.5}$ (79.85) are almost the same, and so for altered ilmenite phases in which the iron is predominantly ferric (e.g. pseudorutile, leucoxene), the TiO_2 content (wt. %) is closely approximated by Ti/(Ti+Fe) × 100.

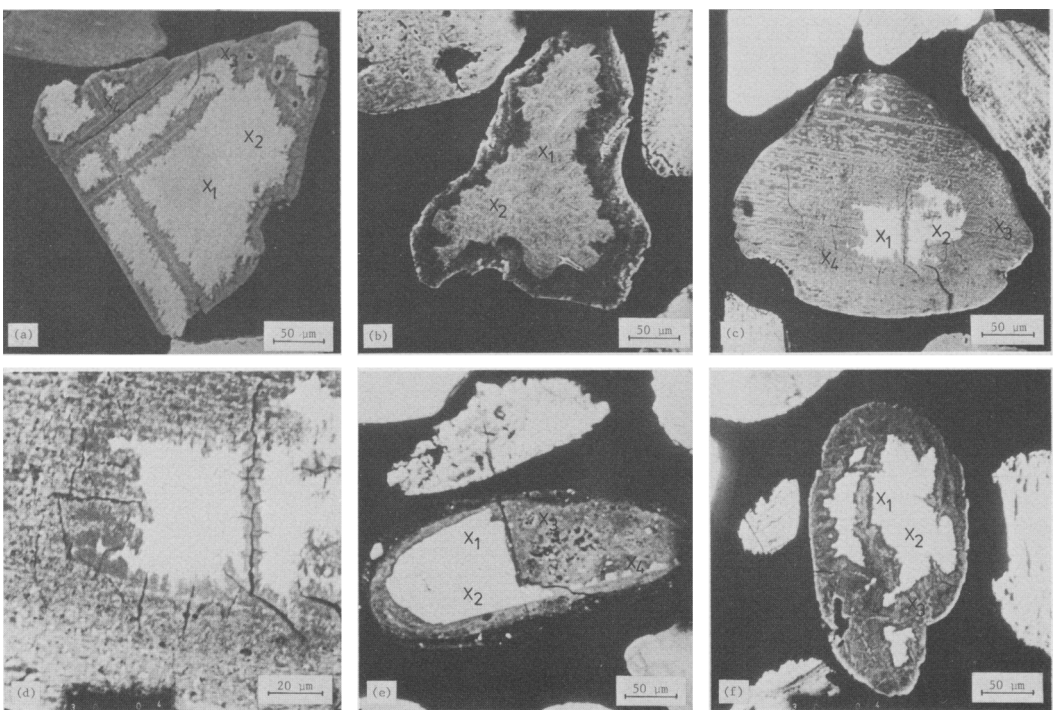

FIG. 1. Backscattered electron images of altered ilmenite grains. (*a*) Grain 5 in Table IV; (*b*) Grain 7 in Table IV; (*c*) and (*d*) Grain 3 in Table III; (*e*) Grain 7 in Table III; (*f*) Grain 5 in Table III. Crosses mark the points analysed, in the order shown in the Tables.

Table II. Distribution of alteration phases from microprobe scans.

	Y.E.-150		Y.E.-90		Eneabba	
Ti/(Ti+Fe)	wt. percent	cumulative	wt. percent	cumulative	wt. percent	cumulative
0.45-0.50	13.9	13.9	3.2	3.2	0.4	0.4
0.51-0.55	32.2	46.1	21.9	25.1	3.0	3.4
0.56-0.60	22.5	68.6	32.5	57.6	14.7	18.1
0.61-0.65	12.5	81.1	28.7	86.3	44.2	62.3
0.66-0.70	9.1	90.2	7.6	93.9	23.1	85.4
0.71-0.75	4.6	94.8	3.3	97.2	7.3	92.7
0.76-0.80	1.5	96.3	1.2	98.4	2.7	95.4
0.81-0.85	2.2	98.5	1.1	99.5	1.5	96.9
0.86-0.90	1.1	99.6	0.5	100.0	0.1	97.0
0.91-0.95	0.4	100.0	-		0.3	97.3
0.96-1.00	-				2.7	100.0

Ti/Ti+Fe)	Alteration stage	Phases present*	Y.E.-150	Y.E.-90	Eneabba
<0.5	1. Ferrian ilmenite	Ferrian ilmenite	13.9	3.2	0.4
0.5-0.6	2. Hydrated ilmenite	Ilmenite + pseudorutile (trace H-239)	54.7	54.4	17.7
0.6-0.7	3. pseudorutile	pseudorutile (+ trace hematite)	21.6	36.3	67.3
0.7-1.0	4. Leucoxene	Pseudorutile + rutile	9.8	6.1	14.6

*Determined from single-crystal XRD studies on Eneabba grains. Preliminary studies on Y.E.-150 grains show rutile present in all stages.

In addition to the (apparently) homogeneous grains, which constituted the bulk of the samples studied, a variety of intra-grain phase associations were observed. SEM/EDS studies showed that for the YE-150 sample, more than 10% of the grains comprised relatively unaltered ilmenite or ferrian-ilmenite cores, with $Ti/(Ti+Fe) \gtrsim 0.5$ surrounded by rims of leucoxene with Ti/(Ti + Fe) in the range 0.7–0.9. Similar ilmenite-leucoxene associations were also observed in the YE-90 and Eneabba grains but they were less common (< 5%). In the latter two samples, the most common associations were pseudorutile with patches and stringers of remnant ilmenite or of leucoxene. A feature occasionally observed in the YE-150 sample was the presence of unaltered ilmenite grains surrounded by a thick coating of material rich in aluminium, silicon, and iron. Electron micrographs showing these various features are presented in fig. 1.

Composition distributions. The distribution of alteration phases is given in Table II, as the percentage of phases having Ti/(Ti + Fe) atomic fractions within the ranges 0.45–0.50, 0.51–0.55, etc.

The data in Table II illustrate the different composition characteristics of the 150-foot strand and the 90-foot strand material. The former is characterized by relatively higher proportions of material at both extremes of the composition range and lower quantities of intermediate alteration phases. The Eneabba ilmenite has a sharp symmetrical composition profile, with a maximum at Ti/(Ti + Fe) = 0.63, reflecting the greater extent of alteration of this material. The small peak in the Ti/(Ti + Fe) range 0.9–1.0 is due to primary rutile.

At the bottom of Table II, the data have been grouped into ilmenite alteration stages according to their Ti/(Ti + Fe) values. The three samples display quite different composition distributions; e.g. the 150-foot strand material shows a relatively high level of ferrian ilmenite, with 14% of the material having Ti/(Ti + Fe) < 0.5, whereas the other two samples have less than 4% in this range. The proportions of hydrated ilmenite are similar for the two Capel samples whereas the Eneabba sample has only one-third as much material remaining in this early stage of alteration, in which residual ilmenite remains in intimate association with pseudorutile.

The samples show markedly different proportions of the material in intermediate alteration

stage pseudorutile, with 22%, 36%, and 67% for YE-150, -90, and Eneabba respectively, reflecting increasing extent of alteration in this order. From LOI experiments on pseudorutile concentrates obtained by magnetic separation we find that there is a continuous increase in strongly held water content (hydroxyls) with increasing Ti/(Ti + Fe), see also Flinter (1959) and Gevork'yan and Tananaev (1964). This may be explained by concomitant hydroxylation and leaching of iron, as given by the reaction:

$$Fe_2Ti_3O_9 + 0.75H_2O \rightarrow Fe_{1.5}Ti_3O_{7.5}(OH)_{1.5} + 0.5FeO_{1.5}. \quad (1)$$

The oriented hematite XRD patterns observed in single-grain XRD studies on samples from this composition region are probably due to reactions similar to (1).

Further detailed studies are needed on the relationship between iron contents and water contents in this composition region to check the proposed reaction and the lower composition limit of single-phase pseudorutile.

The leucoxene contents of the three samples appear to be inconsistent with their relative extents of alteration. As discussed above, the figures for the hydrated-ilmenite and pseudorutile fractions indicate that the extent of alteration increases from YE-150 to YE-90 to Eneabba ilmenite and so the leucoxene values are expected to increase in this order. However the leucoxene content of YE-150, 10%, is higher than that of YE-90, 6%. This may be explained by a different mechanism of alteration for YE-150. As noted in the previous section, SEM studies showed that a proportion of grains in the 150-foot strand material comprised ferrian-ilmenite cores with leucoxene rims, i.e. these grains had altered directly to leucoxene in a single-step dissolution and reprecipitation process without the intermediate formation of pseudorutile. Preliminary single-crystal XRD studies on YE-150 show that small amounts of rutile are present in all four stages of alteration, in contrast to Eneabba ilmenite, where rutile was observed only in stage 4 grains, Table II.

Electron-microprobe analyses. The results of electron-microprobe analyses for Ti, Fe, Al, and Si in individual phases in selected grains are given in Tables III–V for YE-150, YE-90, and Eneabba samples respectively. The grains were selected from SEM examination to contain pairs of coexisting stages, as shown in fig. 1.

The most striking result apparent from a study of Tables III–V is the jump in Al and Si contents in going from ferrian ilmenite and hydrated ilmenite to pseudorutile and leucoxene. In the former alteration stages, the minor element levels are essentially independent of Ti/(Ti + Fe) and vary over quite narrow ranges, 0.1–0.3 wt. % Al_2O_3 and 0–0.1 wt. % SiO_2. In the latter, more highly altered materials, the Al and Si contents are considerably higher and are dependent on the Ti/(Ti + Fe) ratio. Although the results show considerable scatter, a general trend is apparent of increasing Al_2O_3 and SiO_2 contents with increasing Ti/(Ti + Fe), rising to maxima near 3 wt. % Al_2O_3 and 1 wt. % SiO_2 for iron-free leucoxene. This dependence of impurity levels on extent of alteration was examined in more detail using the automated modal-analysis procedure described in the experimental section. The results are presented as plots of impurity content versus composition in figs. 2*a–c* (Al_2O_3) and 3*a–c* (SiO_2). The composition axis is linear in Fe/Ti atomic ratio, to spread out the data for the early alteration stages.

The results reinforce the conclusions drawn from the individual microprobe analyses of Tables III–V and show that the three samples display the same type of behaviour, i.e. for Ti/(Ti + Fe) below about 0.6, the Al and Si contents lie in a narrow range, 0.1–0.3 wt. % Al_2O_3, 0–0.1 wt. % SiO_2, and are virtually independent of the composition. For Ti/(Ti + Fe) > 0.6 there is a fanning-out of the distribution of both elements and the mean value increases with increasing Ti/(Ti + Fe). Linear extrapolation to Ti/(Ti + Fe) = 1 gives Al_2O_3 and SiO_2 values for the three samples in the range 2.5–3 wt. % and 0.5–1 wt. % respectively. These levels cannot be explained simply by the enrichment of the original Al and Si in the grains due to removal of Fe. The high levels observed indicate that extra Al and Si have been incorporated into the grains from the surrounding environment during the alteration process. The extent of incorporation of both elements has an inverse correlation with the Fe content and a positive correlation with the Ti content of the alteration phases.

Mechanism for aluminium and silicon incorporation. The observed dependence of Al and Si contents on Ti/(Ti + Fe) may be explained by the two-stage alteration mechanism for ilmenite proposed by Grey and Reid (1975). According to this model, the first stage of alteration is an electrochemical corrosion process, operating in a groundwater situation, which results in the oxidation of all ferrous iron to ferric, together with diffusion of one third of the ferric ions out of the ilmenite lattice. The overall reaction is:

$$3Fe^{2+}TiO_3 + \tfrac{3}{4}O_2 + \tfrac{3}{2}H_2O \rightarrow Fe_2^{3+}Ti_3O_9 + Fe(OH)_3. \quad (2)$$

This stage results in the formation of the pseudorutile composition, which corresponds to the maximum removal of Fe from the ilmenite structure

Table III. Electron microprobe analyses for Y.E.-150 ilmenite sample.

Grain No.	Coexisting alteration stages	Wt.% of oxides					
		TiO_2	FeO	Al_2O_3	SiO_2	Total	Ti/Ti+Fe)
1.	ferrian ilmenite + leucoxene	51.22*	48.44	0.17	0.01	99.83	0.49
		50.89	48.36	0.15	0.02	99.42	0.49
		77.10	18.07	1.77	0.44	97.38	0.79
		73.64	21.20	1.53	0.41	96.78	0.76
2.	hydrated ilmenite + leucoxene	56.07	45.59	0.23	0.03	101.92	0.53
		56.23	45.41	0.27	0.02	101.93	0.53
		72.58	24.43	0.64	0.53	98.18	0.72
		71.59	22.01	0.77	0.54	94.91	0.75
3.	hydrated ilmenite + leucoxene	55.23	38.90	0.18	0.03	94.34	0.56
		53.96	39.64	0.19	0.03	93.82	0.55
		74.23	20.55	2.59	0.47	97.84	0.76
		75.68	21.13	2.54	0.42	99.77	0.76
4.	hydrated ilmenite + leucoxene	53.72	45.24	0.11	0.02	99.09	0.52
		53.80	45.79	0.10	0.00	99.69	0.51
		88.41	7.85	2.75	0.32	96.83	0.91
		81.22	12.99	0.98	0.23	95.42	0.85
5.	hydrated ilmenite + leucoxene	55.91	42.72	0.16	0.02	98.81	0.54
		54.92	43.21	0.15	0.00	98.28	0.53
		87.05	7.73	1.80	0.12	96.70	0.91
		72.96	10.48	1.28	0.12	84.84	0.86
6.	hydrated ilmenite + pseudorutile	55.87	45.13	0.17	0.06	101.23	0.53
		55.93	44.60	0.16	0.03	100.72	0.53
		64.00	34.53	1.07	0.12	99.72	0.63
		66.41	32.23	0.92	0.07	99.63	0.65
7.	ilmenite + alumino-silicate	52.61	46.96	0.16	0.03	99.76	0.50
		52.79	46.86	0.10	0.00	99.75	0.50
		14.59	42.28	31.05	10.41	98.33	
		5.29	43.50	36.33	12.98	98.10	

*Each pair of point analyses taken from separate regions of the same phase, at least 20 μm apart.

Table IV. Electron microprobe analyses for Y.E.-90 ilmenite sample.

Grain No.	Coexisting alteration stages	Wt.% of oxides					
		TiO_2	FeO	Al_2O_3	SiO_2	Total	Ti/(Ti+Fe)
1.	ilmenite + hydrated ilmenite	52.00	46.99	0.25	0.00	99.24	0.50
		58.48	39.13	0.29	0.07	97.97	0.57
		57.36	39.50	0.33	0.08	97.28	0.56
2.	ilmenite + ferrian ilmenite	51.36	45.99	0.31	0.05	97.72	0.50
		49.54	49.16	0.32	0.02	99.04	0.48
		50.12	48.60	0.23	0.00	98.96	0.48
3.	hydrated ilmenite + leucoxene	57.93	43.42	0.32	0.03	101.70	0.55
		55.46	43.18	0.32	0.06	99.02	0.53
		94.15	4.92	0.56	0.16	99.79	0.94
		72.69	17.28	4.08	4.18	98.23	0.79
4.	ferrian ilmenite + leucoxene	51.23	49.05	0.15	0.04	100.47	0.48
		85.60	6.51	2.42	0.56	95.09	0.93
5.	hydrated ilmenite + leucoxene	56.06	40.16	0.29	0.11	96.62	0.56
		56.48	40.65	0.29	0.10	97.53	0.56
		76.44	12.75	2.05	0.75	91.98	0.84
		74.13	16.52	1.77	0.54	92.96	0.80
6.	ilmenite + pseudorutile	50.42	46.27	0.16	0.00	96.85	0.50
		51.30	46.03	0.15	0.02	97.51	0.50
		59.21	31.88	1.22	0.48	92.80	0.63
		57.64	33.67	1.14	0.67	93.13	0.61
7.	pseudorutile + leucoxene	62.63	33.70	1.16	0.08	97.57	0.63
		60.77	34.93	0.96	0.09	96.76	0.61
		74.30	16.97	3.28	0.51	95.06	0.80
		73.65	19.87	2.95	0.41	96.87	0.77
8.	ilmenite + leucoxene	51.72	44.85	0.22	0.04	96.83	0.51
		51.73	46.44	0.22	0.05	98.44	0.50
		79.90	7.29	2.54	1.07	90.81	0.91
		73.47	16.39	2.14	1.03	93.04	0.80

Table V. Electron microprobe analyses for Eneabba ilmenite sample.

Grain No.	Coexisting alteration stages	Wt.% of oxides					
		TiO_2	FeO	Al_2O_3	SiO_2	Total	(Ti/(Ti+Fe)
1.	ilmenite + leucoxene	52.75	47.45	0.12	0.02	100.34	0.50
		52.45	47.07	0.12	0.00	99.64	0.50
		65.55	26.58	0.81	0.63	93.57	0.69
2.	ferrian-ilmenite + leucoxene	46.68	52.68	0.25	0.03	99.64	0.44
		46.94	53.96	0.21	0.02	101.13	0.44
		69.30	18.12	1.13	0.93	89.48	0.78
		63.69	15.23	1.10	0.96	80.98	0.79
3.	leucoxene	68.76	24.66	0.64	0.44	94.50	0.71
		65.39	15.71	0.80	0.75	82.65	0.79
4.	pseudorutile	63.95	33.30	0.82	0.31	98.38	0.63
		62.47	36.58	0.61	0.22	99.88	0.61
		62.73	35.31	0.71	0.27	99.02	0.61
5.	hydrated ilmenite + ferrian-ilmenite	57.08	39.19	0.30	0.37	96.94	0.57
		55.06	40.75	0.31	0.32	96.44	0.55
		50.14	48.28	0.23	0.01	98.66	0.48
		50.47	47.17	0.23	0.00	97.87	0.49
6.	pseudorutile	58.44	33.30	3.12	3.34	98.20	0.61
		56.69	36.59	1.71	1.64	96.63	0.58
		56.81	33.90	3.18	3.66	97.55	0.60

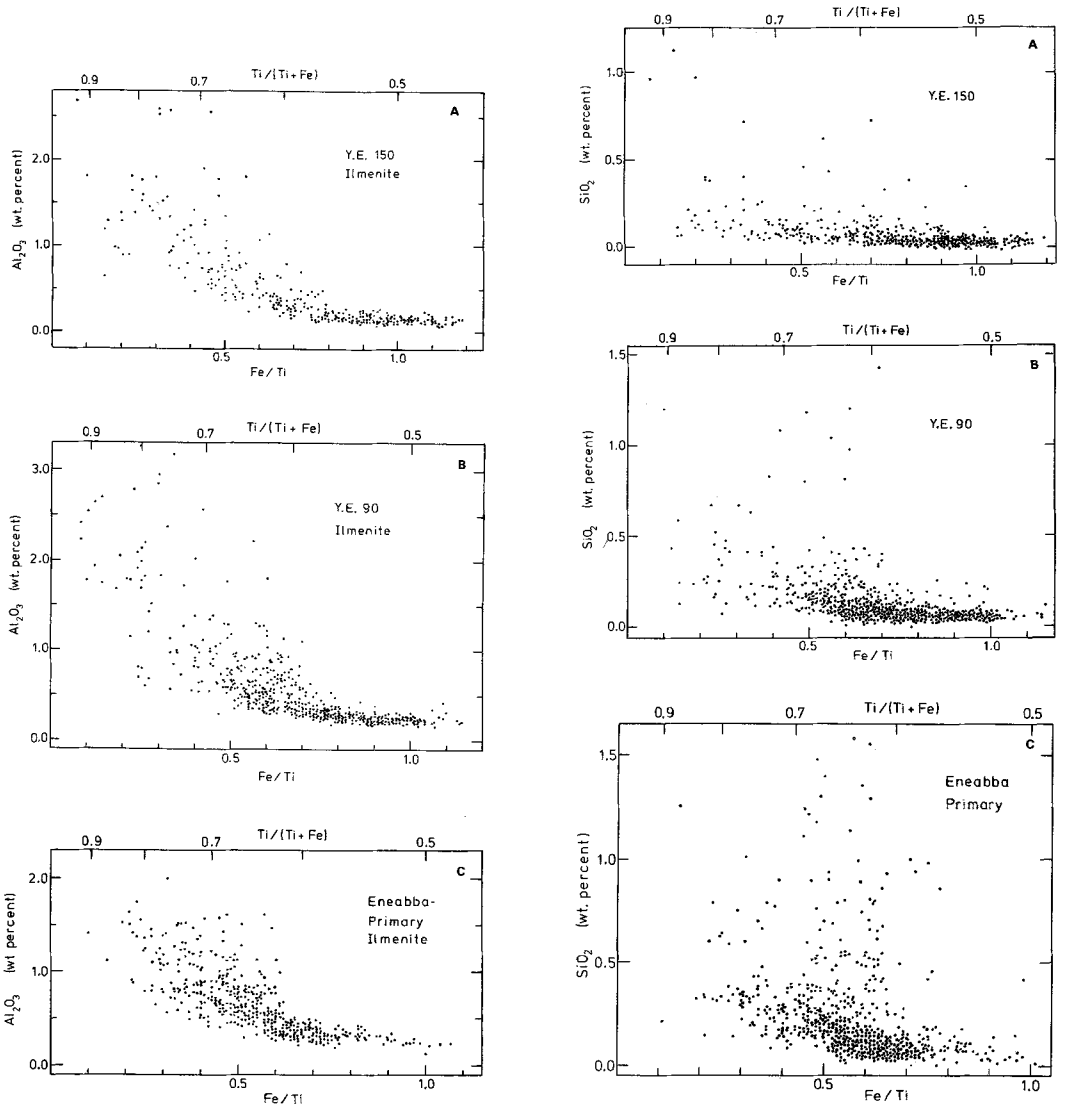

FIGS. 2 and 3. FIG. 2 (*left*). Variation of aluminium content, as Al_2O_3, with Fe/Ti atomic ratio in altered ilmenite grains. (*a*) YE-150, (*b*) YE-90, (*c*) Eneabba ilmenite. FIG. 3 (*right*). Variation of silicon content, as SiO_2, with Fe/Ti atomic ratio in altered ilmenite grains. (*a*) YE-150, (*b*) YE-90, (*c*) Eneabba ilmenite.

without concomitant removal of oxygen, i.e. the anion lattice remains intact during this stage and no bulk dissolution of the ilmenite occurs. Impurities in the ilmenite such as Al and Si, which do not participate in the electrochemical alteration, will be slightly enriched due to the Fe depletion. Thus, during the first stage of alteration, as the Ti/(Ti + Fe) is increased to 0.60 (pseudorutile), the Al and Si contents increase only very slightly, as observed in figs. 2 and 3.

Further removal of Fe beyond the pseudorutile composition involves removal of oxygen also, leading eventually to rutile according to the reaction:

$$Fe_2Ti_3O_9 \rightarrow 3TiO_2 + Fe_2O_3. \qquad (3)$$

Thus the second stage of alteration involves a disruption of the anion lattice as both iron and oxygen are removed. This stage proceeds via a leaching and reprecipitation mechanism, in mildly reducing acidic solutions, of the type that is commonly associated with the near-surface zones of

lateritic and bauxitic deposits. Under these conditions, iron titanates undergo incongruent dissolution; the Fe stays in solution whereas the Ti reprecipitates back on to the original grains as a colloidal hydrated oxide. If the surrounding solution contains high enough concentrations of Al and Si ions, e.g. from the decomposition of clays, then, for suitable pH conditions, these will coprecipitate with the Ti or be adsorbed on to the colloid surface, leading to increases in the Al and Si contents in the alteration products, as experimentally observed.

The mechanism for the second stage of alteration needs to be modified from that described by Grey and Reid (1975) to allow for hydration (hydroxylation) of the intermediate alteration phases (Flinter, 1959; Gevork'yan and Tananaev, 1964). This can result in an extended range of homogeneity of pseudorutile and reactions similar to (1) probably occur, in which the anion lattice remains intact and hydrogen replaces iron in the octahedral interstices of the anion framework. This type of mechanism has recently been proposed for the formation of the hydrated ferric titanate mineral, kleberite (Bautsch, *et al.*, 1978). The extent of hydration is also presumably related to the alumina and silica contents (cf. hydrohematite, in which trace amounts of Al increase the extent of hydroxylation by 50% (Wolska, 1981)). From the results presented in Tables III–V, it is seen that a significant increase occurs in the Al and Si levels in the pseudorutile phase relative to those in hydrated ilmenite. However the increase is not as dramatic as that observed in going from pseudorutile to leucoxene, where bulk dissolution and reprecipitation takes place. A similar dependence of hydration on the extent of alteration is apparent from an analysis of the results of Flinter (1959) and Gevork'yan and Tananaev (1964).

It is apparent from the wide scatter in the Al and Si levels above $Ti/(Ti+Fe) = 0.6$ (figs. 2 and 3) that the individual grains have been subjected to different local environments during their alteration history. The extent of incorporation of Al and Si will depend on many factors, including the concentration of these ions in solution, pH, E_h, and temperature of the solution. These factors in turn will control the mechanism of Fe removal in the pseudorutile–leucoxene composition regions, e.g. by direct dissolution of pseudorutile with reprecipitation of leucoxene, or by progressive hydration and leaching. Further work is needed to determine the relationships between the mechanisms for hydration and Fe removal and those for Si and Al incorporation.

Acknowledgements. We thank Westralian Sands Limited for supporting the studies reported here and for supplying samples of ilmenite from Capel, WA. We thank also Associated Minerals Consolidated for supplying a sample of Eneabba primary ilmenite, together with analyses.

REFERENCES

Bautsch, H. J., Rohde, G., Sedlacek, P., and Zedler, A. (1978) *Z. Geol. Wiss.* **6,** 661–71.

Dyadchenko, M. G., and Khatuntseva, A. Ya. (1960) *Doklady Akad. Nauk SSSR,* **132,** 435–8.

Flinter, B. H. (1959) *Econ. Geol.* **54,** 720–9.

Gevork'yan, V. K., and Tananaev, M. V. (1964) *Dopovidis Akademii Nauk Ukrains'koi RSR,* **10,** 1366–9.

Grey, I. E., and Reid, A. F. (1972) *J. Solid State Chem.* **4,** 186–94.

———(1975) *Am. Mineral.* **60,** 898–906.

———and Allpress, J. G. (1973) *J. Solid State Chem.* **8,** 86–99.

Robinson, V. N. E. (1975) In *Scanning electron microscopy/1975* (O. Johari and I. Corvin, eds.), II TRJ, Chicago, 51–60.

Wolska, E. (1981) *Z. Kristallogr.* **154,** 69–75.

Wort, M. J., and Jones, M. P. (1981) *Trans. Inst. Mining Metall.* (Sect. C) **90,** C130–7.

[*Manuscript received 21 October 1981; revised 19 July 1982*]